Acta Cryst E
CRYSTALLOGRAPHIC COMMUNICATIONS
ISSN 2056-9890

Structural features of the oxidonitridophosphates $K_3M^{III}(PO_3)_3N$ (M^{III} = Al, Ga)

Igor V. Zatovsky,[a]* Ivan V. Ogorodnyk,[b] Vyacheslav N. Baumer,[c] Ivan D. Zhilyak,[d] Ruslana V. Horda[a] and Nataliya Yu. Strutynska[e]

[a]F.D. Ovcharenko Institute of Biocolloidal Chemistry, NAS Ukraine, 42 Acad. Vernadskoho blv., 03142 Kyiv, Ukraine, [b]ShimUkraine LLC, 18 Chigorina Str., office 429, 01042 Kyiv, Ukraine, [c]STC "Institute for Single Crystals", NAS of Ukraine, 60 Lenin ave., 61001 Kharkiv, Ukraine, [d]Faculty of Horticulture, Ecology and Plants Protection, Uman National University of Horticulture, 1 Instytutska str., 20305 Uman, Cherkassy region, Ukraine, and [e]Department of Inorganic Chemistry, Taras Shevchenko National University of Kyiv, 64/13, Volodymyrska str., 01601, Kyiv, Ukraine. *Correspondence e-mail: zvigo@yandex.ru_&_zvigo@ukr.net

Received 11 October 2021
Accepted 27 October 2021

Edited by M. Weil, Vienna University of Technology, Austria

Keywords: crystal structure; isotypism; $(PO_3)_3N$ anion; cubic symmetry; self-flux crystal growth.

CCDC references: 2118192; 2118191

Supporting information: this article has supporting information at journals.iucr.org/e

Cubic crystals of tripotassium aluminium (or gallium) nitridotriphosphate, $K_3M^{III}(PO_3)_3N$ (M^{III} = Al, Ga), were grown by application of the self-flux method. In their isostructural crystal structures, all metal cations and the N atom occupy special positions with site symmetry 3, while the P and O atoms are situated in general positions. The three-dimensional framework of these oxidonitridophosphates is built up from $[M^{III}O_6]$ octahedra linked together *via* $(PO_3)_3N$ groups. The latter are formed from three PO_3N tetrahedra sharing a common N atom. The coordination environments of the three potassium cations are represented by two types of polyhedra, *viz*. KO_9 for one and KO_9N for the other two cations. An unusual tetradentate type of coordination for the latter potassium cations by the $(PO_3)_3N^{6-}$ anion is observed. These $K_3M^{III}(PO_3)_3N$ (M^{III} = Al, Ga) compounds are isostructural with the $Na_3M^{III}(PO_3)_3N$ (M^{III} = Al, V, Ti) compounds.

1. Chemical context

Oxidonitridophosphates with general compositions $M^{I}_3M^{III}(PO_3)_3N$ and $M^{I}_2M^{II}_2(PO_3)_3N$ (M^{I} = Li, Na, K; M^{III} = Al, Cr, Ga, V and Ti; M^{II} = Mg, Fe) have been prepared by solid-state synthesis (Feldmann, 1987*a*,*b*; Massiot *et al.*, 1996; Conanec *et al.*, 1996), high-temperature thermal ammonolysis (Kim & Kim, 2013; Kim *et al.*, 2017; Zhang *et al.*, 2017), flux-growth (Zatovsky *et al.*, 2006) or solid–solid ion-exchange (Liu *et al.*, 2018). In recent years, oxidonitridophosphates containing the $(PO_3)_3N^{6-}$ anion have been intensively studied as promising cathode materials for Na-ion and Li-ion batteries. In particular, ionic conductivities and redox properties were investigated in detail for $Na_3Ti(PO_3)_3N$ (Liu *et al.*, 2014), $Na_3V(PO_3)_3N$ (Reynaud *et al.*, 2017; Kim *et al.*, 2017; Zhang *et al.*, 2017; Xiao *et al.*, 2021; Wang *et al.*, 2021), $Li_3V(PO_3)_3N$ (Liu *et al.*, 2018), $Na_2Fe_2(PO_3)_3N$ and $Li_2Fe_2(PO_3)_3N$ (Liu *et al.*, 2013), $Na_2Mg_2(PO_3)_3N$ (Cosby *et al.*, 2020), and $Li_2Mg_2(PO_3)_3N$ (Liu *et al.*, 2017). In addition, rare-earth-doped $Na_3Al(PO_3)_3N$ has been studied as a promising phosphor (Bang *et al.*, 2013). However, the structural data for oxidonitridophosphates include only Na- or Li-containing compounds (Massiot *et al.*, 1996; Zatovsky *et al.*, 2006; Kim & Kim, 2013; Liu *et al.*, 2013, 2017, 2018; Zhang *et al.*, 2017).

In this communication, we report the flux-growth synthesis, structural characterization and FTIR spectra for the two

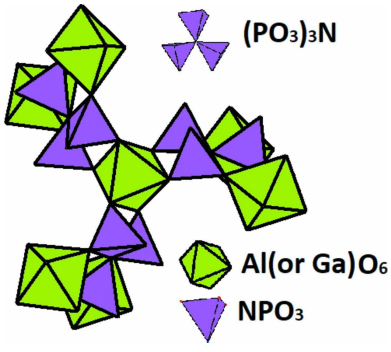

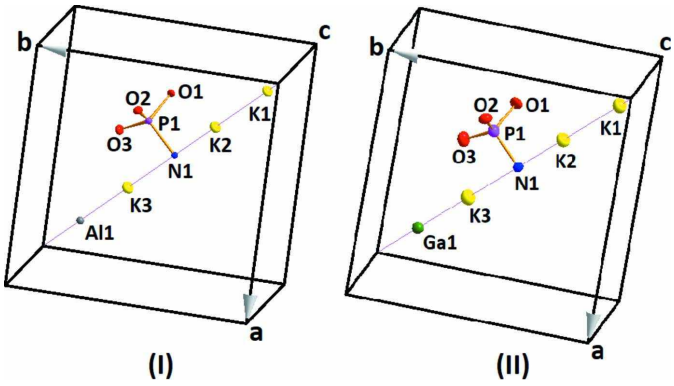

Figure 1
A view of the asymmetric units of $K_3Al(PO_3)_3N$ (I) and $K_3Ga(PO_3)_3N$ (II), with displacement ellipsoids drawn at the 50% probability level.

K-containing oxidonitridophosphates $K_3Al(PO_3)_3N$ (I) and $K_3Ga(PO_3)_3N$ (II).

2. Structural commentary

Compounds (I) and (II) (Fig. 1) are isotypic and crystallize in the cubic $Na_3Al(PO_3)_3N$ structure in space-group type $P2_13$. The K, Al (or Ga) and N atoms are localized on threefold rotation axes (Wyckoff position 4 *a*), and the P and all O atoms occupy general 12 *b* sites (Fig. 1). As shown in Fig. 2, the crystal structures of the $K_3M^{III}(PO_3)_3N$ (M^{III} = Al, Ga) title compounds consist of $[M^{III}O_6]$ octahedra and $(PO_3)_3N^{6-}$ anions, which are linked *via* vertices, forming a three-dimensional framework. The $(PO_3)_3N^{6-}$ anion is built up from three PO_3N tetrahedra sharing a common N vertex atom. The P—O bond lengths for both structures range between 1.473 (9) and 1.534 (3) Å (Tables 1 and 2), while the P—N bond lengths are 1.7084 (12) and 1.701 (4) Å for (I) and (II), respectively. The lengths of the P—O and P—N bonds are similar to those

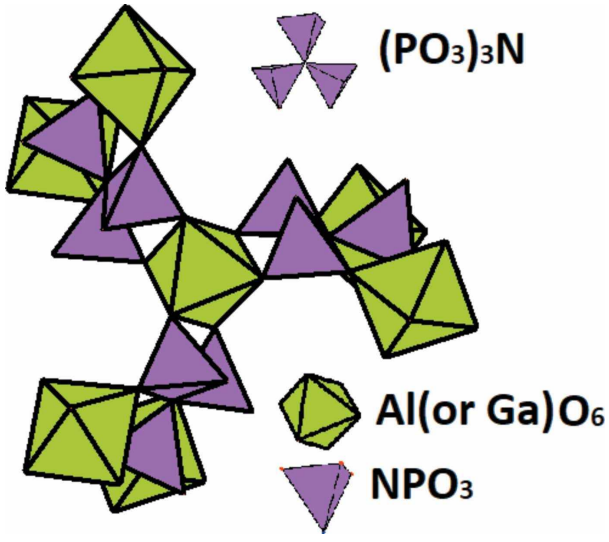

Figure 2
$[M^{III}O_6]$ octahedra and 'three-blade propeller'-type anions $(PO_3)_3N^{6-}$ as principle building units for formation of the three-dimensional framework of (I) and (II).

Table 1
Selected geometric parameters (Å, °) for (I).

K1—O3^{i}	2.623 (3)	K3—N1	3.340 (6)
K1—O1^{ii}	2.761 (3)	K3—O3^{iv}	3.379 (3)
K1—O2^{ii}	3.261 (3)	Al1—O1^{v}	1.905 (3)
K2—O3^{iii}	2.765 (3)	Al1—O2^{iv}	1.909 (3)
K2—N1	2.904 (6)	P1—O3	1.493 (3)
K2—O1^{iii}	2.967 (3)	P1—O1	1.530 (3)
K2—O2	3.263 (3)	P1—O2	1.534 (3)
K3—O3	2.679 (3)	P1—N1	1.7084 (12)
K3—O2^{iv}	2.803 (3)		
O3—P1—O1	111.58 (17)	O1—P1—N1	105.82 (13)
O3—P1—O2	113.45 (16)	O2—P1—N1	105.20 (17)
O1—P1—O2	109.85 (16)	P1^{vi}—N1—P1	118.53 (8)
O3—P1—N1	110.5 (2)		

Symmetry codes: (i) $-y+1, z-\frac{1}{2}, -x+\frac{1}{2}$; (ii) $-z+\frac{1}{2}, -x, y-\frac{1}{2}$; (iii) $z-\frac{1}{2}, -x+\frac{1}{2}, -y+1$; (iv) $-z+1, x+\frac{1}{2}, -y+\frac{3}{2}$; (v) $-z+\frac{3}{2}, -x+1, y+\frac{1}{2}$; (vi) z, x, y.

Table 2
Selected geometric parameters (Å, °) for (II).

K1—O3^{i}	2.642 (8)	K3—N1	3.310 (18)
K1—O1^{ii}	2.807 (9)	K3—O3^{v}	3.412 (8)
K1—O2^{iii}	3.216 (8)	Ga1—O2^{vi}	1.968 (9)
K2—O3^{iv}	2.808 (9)	Ga1—O2^{vii}	1.968 (9)
K2—O1^{i}	2.925 (9)	P1—O3	1.473 (9)
K2—N1	2.977 (18)	P1—O2	1.516 (9)
K2—O2	3.287 (8)	P1—O1	1.524 (9)
K3—O3	2.665 (9)	P1—N1	1.701 (4)
K3—O2^{v}	2.785 (8)		
O3—P1—O2	113.8 (5)	O2—P1—N1	107.0 (5)
O3—P1—O1	112.1 (5)	O1—P1—N1	106.8 (4)
O2—P1—O1	107.9 (5)	P1—N1—P1^{viii}	118.8 (2)
O3—P1—N1	108.9 (7)		

Symmetry codes: (i) $z-\frac{1}{2}, -x+\frac{1}{2}, -y+1$; (ii) $-x, y-\frac{1}{2}, -z+\frac{1}{2}$; (iii) $-z+\frac{1}{2}, -x, y-\frac{1}{2}$; (iv) $-y+1, z-\frac{1}{2}, -x+\frac{1}{2}$; (v) $-z+1, x+\frac{1}{2}, -y+\frac{3}{2}$; (vi) $-y+\frac{3}{2}, -z+1, x+\frac{1}{2}$; (vii) $x+\frac{1}{2}, -y+\frac{3}{2}, -z+1$; (viii) z, x, y.

found in the isotypic oxidonitridophosphates such as $Na_3Al(PO_3)_3N$ (Conanec *et al.*, 1994, 1996), $Na_3Ti(PO_3)_3N$ (Zatovsky *et al.*, 2006), or $Na_3V(PO_3)_3N$ (Kim & Kim, 2013). The octahedral coordination environments around M^{III} are slightly distorted, as indicated by the different M^{III}—O bond lengths (Tables 1 and 2). The $[M^{III}O_6]$ octahedra are slightly squeezed along the cubic cell diagonal. The average Al—O and Ga—O distances are 1.907 (3) and 1.963 (9) Å, respectively. These values are close to the sums of the ionic radii (Shannon, 1976) of Al^{3+} and O^{2-} (1.92 Å) and Ga^{3+} and O^{2-} (2.00 Å), respectively.

Fig. 3 shows the coordination environments of potassium cations for (I) and (II). K1 has nine O-atom neighbors with

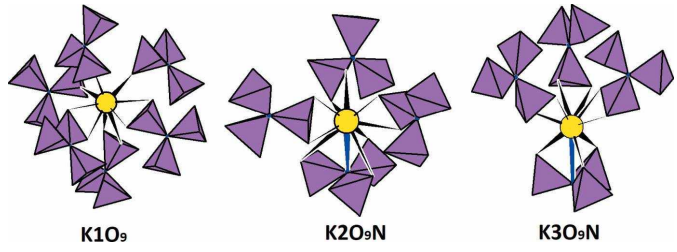

Figure 3
The coordination environment of potassium cations in (I) and (II).

Table 3
BVS results (v.u.) for (I) and (II).

Central Atom	(I)	(II)
Al1/Ga1	3.004	3.197
K1	1.486	1.400
K2	1.122	1.069
K3	1.315	1.360
P1	3 × 4.903	3 × 5.084
Σ	21.636	22.278

K—O distances ranging from 2.623 (3) to 3.261 (3) Å, which includes three mono- and three bidentately coordinating $(PO_3)_3N^{6-}$ anions. $K2O_9N$ and $K3O_9N$ polyhedra are formed as a result of one tetra- and three bidentately coordinating oxidonitridophosphate anions. In the latter case, the upper boundary for K—O distances is 3.412 (8) Å; K2—N distances are 2.904 (6) and 2.977 (18) Å and K3—N contacts are 3.340 (6) and 3.310 (18) Å for (I) and (II), respectively. The coordination environments around the alkali metal for K-containing oxidonitridophosphates ($K2O_9N$ and $K3O_9N$ polyhedra) differ from those of the Na-containing compounds ($Na2O_6N$ and $Na3O_6N$ polyhedra). In addition, the $(PO_3)_3N^{6-}$ anions coordinate the two potassium cations in a tetradentate manner (Fig. 4). As is shown schematically in Fig. 4 and in Table 3 for the isotypic $M^{I}{}_3M^{III}(PO_3)_3N$ compounds, the M^{I}, M^{III} and N atoms are arranged along the [111] direction in the sequence $-M1^{I}-M2^{I}-N-M3^{I}-M^{III}-M1^{I}-$ whereby the $M2^{I}$—N—$M3^{I}$ distances change in a different manner. In case of (I) and (II), the shape of the $(PO_3)_3N^{6-}$ anion is similar (the P—N distances are about 1.70 Å and the P—N—K3 angles are within 83-84°; Tables 1 and 2). For the Na-containing analogues, the P—N bond is slightly larger (1.71–1.74 Å) and the P—N—Na3 angles are smaller within a wider range from 75 to 78° (Conanec *et al.*, 1994, 1996; Zatovsky *et al.*, 2006; Kim & Kim, 2013).

To clarify some points regarding the structural changes we have calculated the bond-valence sums (BVS) for the K, P and Al atoms (I) and Ga atoms (II), respectively. Parameters were taken from Brown & Altermatt (1985) and for the K—N bond from Brese & O'Keeffe (1991). The BVS for positively charged atoms in (I) is 21.64 v.u. and 22.28 v.u. for (II) while the sum of the charges of nine O and one N atom is equal to 21 v.u. (Table 4). The higher values for the Ga-containing compound might be explained as follows. The BVS for Al in $[AlO_6]$ was found to be 3.00 v.u. while for Ga in $[GaO_6]$ it is 3.20 v.u. The remaining atoms also show a slight overbonding (Table 4). We suppose that the anionic part $(PO_3)_3N^{6-}$ is rigid enough and cannot be stretched to larger sizes relative to the larger $[GaO_6]$ octahedron into a more expanded framework. This is the reason why shorter interatomic K—O and P—O distances are observed in the structure of (II) compared to that of (I) (Tables 1 and 2). As expected, the unit-cell parameters of (I) are smaller than for (II), in good agreement with the ionic radii of Al^{3+} and Ga^{3+} (Shannon, 1976). In other words, the rigid and almost flat 'three-blade propeller' anions combine with $[M^{III}O_6]$ octahedra to form the framework in which the cavities for the alkali cations become smaller as greater octahedra are involved. Moreover, the greater $[M^{III}O_6]$ octahedra strongly influence the 'three-blade propeller' anion, resulting in slightly shorter P—O and P—N bonds. On the other hand, the local environments of the K cations should also be mentioned. In the $K2O_9N$ polyhedron, the BVS for K2 is 1.12 v.u. in (I) and 1.07 in (II). The contribution to the K2—N1 bond to the valence sum is 0.12 v.u. for (I) and 0.10 for (II). These high values indicate a strong interaction between the two atoms. The cavities in which K1 and K2 are located become larger with longer or almost the same K···O and K···N contacts, while the cavities in which K3 is situated become smaller with shortened K···O contacts in (II) in comparison with (I). BVS calculations for the phosphate tetrahedra show similar results (Table 4).

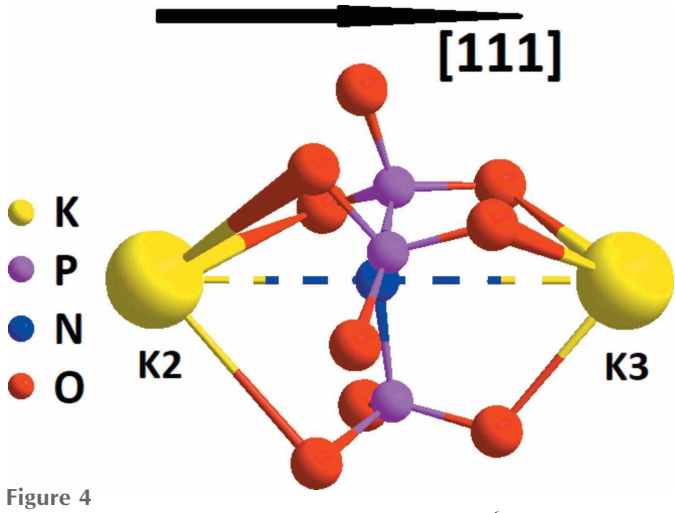

Figure 4
Coordination of K2 and K3 cations by the $(PO_3)_3N^{6-}$ anion for (I) and (II).

It should also be noted that further theoretical calculations of the electronic structure can bring final clarity to the principles of bonding of alkali cations with $(PO_3)_3N^{6-}$ anions in $K_3M^{III}(PO_3)_3N$ compounds. This could be a way for the creation of new materials with desired properties based on K-containing oxidonitridophosphates.

Table 4
Distances (Å) between atoms for (I), (II) and isotypic $M^{I}{}_3M^{III}(PO_3)_3N$ compounds along [111].

Compound	Atomic distance between neighboring atoms	Reference
$Na_3Al(PO_3)_3N$	–Na1–3.438–Na2–2.875–N–3.197–Na3–3.068–Al–3.486–Na1–	Massiot *et al.* (1996)
$Na_3Ti(PO_3)_3N$	–Na1–3.448–Na2–3.078–N–3.188–Na3–3.100–Ti–3.638–Na1–	Zatovsky *et al.* (2006)
$Na_3V(PO_3)_3N$	–Na1–3.477–Na2–2.947–N–3.234–Na3–3.100–V–3.606–Na1–	Kim & Kim (2013)
$K_3Al(PO_3)_3N$	–K1–3.723–K2–2.904–N–3.340–K3–3.400–Al–3.429–K1–	This work
$K_3Ga(PO_3)_3N$	–K1–3.747–K2–2.978–N–3.310–K3–3.350–Ga–3.470–K1–	This work

3. Synthesis and crystallization

For the synthesis of (I) and (II), KH_2PO_4, $K_4P_2O_7{\cdot}10H_2O$, urea, Al_2O_3 or Ga_2O_3 (all analytically or extra pure grade) were used as initial reagents. The sequence of preparation procedure was as follows: (1) phosphates KPO_3 and $K_4P_2O_7$ were each prepared by calcining KH_2PO_4 and $K_4P_2O_7{\cdot}10H_2O$ at 873 K; (2) a mixture of 20.07 g of KPO_3, 13.21 g of $K_4P_2O_7$ and 30.03 g of urea (molar ratio K:P = 1:1.32, urea:P = 2:1) ground in an agate mortar, was heated to complete degassing at 623 K in a porcelain dish. The resulting solid was reground and heated to become a homogeneous liquid at 1023 K and then quenched by pouring the melt onto a copper sheet to form a glass. The glass was crushed using a mill, and a powder with a particle size of less than 125 µm was separated. According to chemical analysis, the prepared glass had the composition $K_{1.32}PO_{2.43}N_{0.50}$; (3) a mixture of 10 g of glass ($K_{1.32}PO_{2.43}N_{0.50}$) and 0.3 g of Al_2O_3 or 0.7 g of Ga_2O_3 powders were placed into porcelain crucibles and heated up to 1043 K and then cooled to 923 K at a rate of 25 K h^{-1}. After cooling to room temperature, colorless tetrahedral crystals of (I) or (II) were washed with deionized water. Elemental analysis indicated the presence of K, Al (or Ga), P and N in the atomic ratio 3:1:3:1.

The growing of well-shaped crystals of (I) and (II) suitable for single crystal X-ray diffraction analysis was one of main tasks during the present study. Hence, a similar way for the preparation of the potassium-containing phosphates to that for the previously reported sodium-containing compounds was applied, following the self-flux method for the preparation of crystalline nitrogen-containing phosphates (Zatovsky *et al.*, 2006). Thermal decomposition of urea is a multistage process and leads to the formation of C_3N_4 (Wang *et al.*, 2017). The initial M^{I}–P–O–N (M^{I} = alkali metal) melt can be obtained by the reaction of urea with alkali metal phosphates, when a mixture of phosphates and C_3N_4 interact. The change of the phosphate:C_3N_4 ratio (or phosphate:urea) and the nature of the alkali metal affects the composition of the resulting melt. In our case, the molar ratio of K:P was chosen to be 1:1.32 because a mixture of KPO_3 and $K_4P_2O_7$ in this ratio has the lowest melting point close to 886 K, and the urea:P ratio was set to 2:1. As a result, a glass of composition $K_{1.32}PO_{2.43}N_{0.50}$ was obtained.

The solubilities of Al_2O_3 and Ga_2O_3 in the $K_{1.32}PO_{2.43}N_{0.50}$ self-fluxes differ significantly. Crystallization of compound (I) occurs as a result of the interaction of self-fluxes and 2–4%wt. Al_2O_3. The formation of a mixture of (I) and Al_2O_3 was observed when the initial amount of aluminum oxide was higher than 5%wt. The solubility of Ga_2O_3 in the self-flux is about 7%wt. at 1043 K, and subsequent cooling of the homogeneous melt led to the crystallization of compound (II). In all cases, the amount of nitrogen in the self-fluxes rapidly decreases above 1063 K. This process occurs due to the thermal instability of P—N bonds at high temperatures, and leads to a redox reaction with the release of nitrogen and phosphorus. The latter vaporizes from the phosphate melts and starts to burn, which can be observed by periodical sparks on the melt surface (Zatovsky *et al.*, 2000). As a result, K–M^{III}–P–O (M^{III} = Al, Ga) melts prone to vitrifying are formed.

The obtained compounds (I) and (II) were further characterized using FTIR spectroscopy; FTIR spectra were collected at room temperature on KBr discs using a Thermo NICOLET Nexus 470 spectrophotometer. As can be seen in Fig. 5, the spectra of (I) and (II) are similar with respect to intensities and band positions (the difference in the band positions does not exceed 27 cm^{-1}). The characteristic bands are in good agreement with the presence of the $N(PO_3)_3^{6-}$ anion with C_{3v} symmetry, which provides for a set of vibration modes: 6A1 + 5*A*2 + 11*E* (3*A*1 + *A*2 + 4*E* belong to stretching vibrations, and 3*A*1 + 4*A*2 + 7*E* are due to deformation vibrations). As shown in Fig. 5, the following regions can be distinguished in the FTIR spectra: (1) the bands in the region between 980 and 1220 cm^{-1} are assigned to ν_{as} and $\nu_s(PO_3)$ stretching vibrations [four absorption bands in the frequency range between 1070 and 1220 cm^{-1} belong to ν_{as}(P—O), and two bands of between 980 and 1060 cm^{-1} correspond to ν_s(P—O)]; (2) ν_{as}(P—N—P) and ν_s(P—N—P) bands can be observed in the regions between 920 and 950 cm^{-1} and around 920 cm^{-1}, respectively; (3) the range between 400 and 680 cm^{-1} includes absorption bands due to δ (P—O) and ν (Al—O) or ν (Ga—O) vibrations. In summary, in terms of the set of absorption bands, the FTIR spectra of the $N(PO_3)_3^{6-}$ anion resemble those of the $P_2O_7^{4-}$ anion.

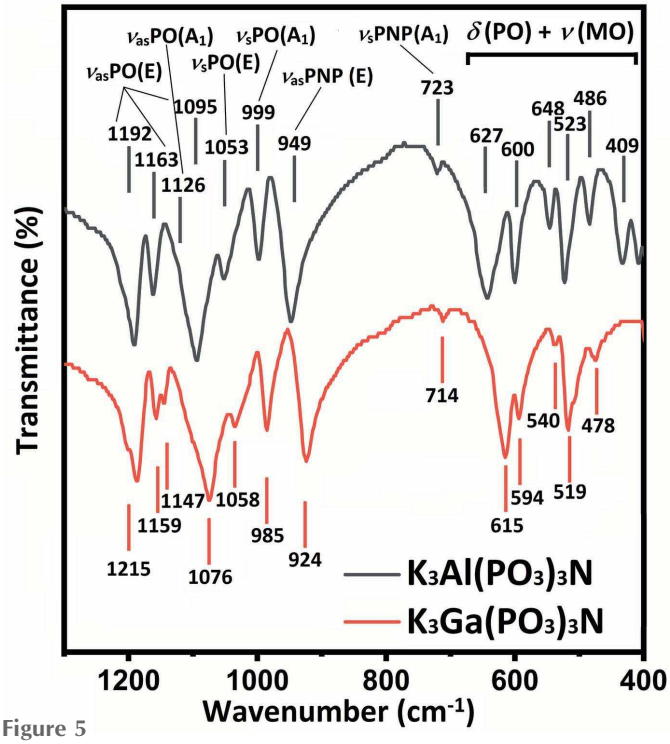

Figure 5
FTIR spectra of (I) and (II).

4. Refinement

Crystal data, data collection and structure refinement details are summarized in Table 5. As a result of the shapes of the obtained crystals, their cell parameters and chemical compo-

Table 5
Experimental details.

	(I)	(II)
Crystal data		
Chemical formula	$K_3Al(NP_3O_9)$	$K_3Ga(NP_3O_9)$
M_r	395.2	437.94
Crystal system, space group	Cubic, $P2_13$	Cubic, $P2_13$
Temperature (K)	293	293
a (Å)	9.6970 (4)	9.7313 (9)
V (Å^3)	911.83 (11)	921.5 (3)
Z	4	4
Radiation type	Mo $K\alpha$	Mo $K\alpha$
μ (mm^{-1})	2.16	4.90
Crystal size (mm)	0.15 × 0.12 × 0.1	0.12 × 0.07 × 0.04
Data collection		
Diffractometer	Oxford Diffraction Xcalibur-3	Oxford Diffraction Xcalibur-3
Absorption correction	Multi-scan (Blessing, 1995)	Multi-scan (Blessing, 1995)
T_{min}, T_{max}	0.844, 0.869	0.738, 0.804
No. of measured, independent and observed [$I > 2\sigma(I)$] reflections	7172, 745, 667	4964, 753, 517
R_{int}	0.078	0.155
$(\sin \theta/\lambda)_{max}$ (Å^{-1})	0.660	0.660
Refinement		
$R[F^2 > 2\sigma(F^2)]$, $wR(F^2)$, S	0.026, 0.052, 1.05	0.059, 0.102, 1
No. of reflections	745	753
No. of parameters	53	53
$\Delta\rho_{max}$, $\Delta\rho_{min}$ (e Å^{-3})	0.27, −0.27	0.67, −0.60
Absolute structure	Flack x determined using 269 quotients $[(I^+)-(I^-)]/[(I^+)+(I^-)]$ (Parsons *et al.*, 2013)	Flack x determined using 153 quotients $[(I^+)-(I^-)]/[(I^+)+(I^-)]$ (Parsons *et al.*, 2013)
Absolute structure parameter	−0.02 (6)	0.03 (5)

Computer programs: *CrysAlis CCD* (Oxford Diffraction, 2006), *CrysAlis RED* (Oxford Diffraction, 2006), *SHELXS* (Sheldrick, 2008), *SHELXS2013/1* (Sheldrick, 2008), *SHELXL2018/3* (Sheldrick, 2015), *DIAMOND* (Brandenburg, 2006), *WinGX* (Farrugia, 2012), *enCIFer* (Allen *et al.*, 2004) and *publCIF* (Westrip, 2010).

sitions, we had expected that both structures should be isostructural with the previously reported $Na_3Al(PO_3)_3N$ and $Na_3Ti(PO_3)_3N$ structures. In fact, analysis of the single-crystal data showed that both compounds crystallize in the same space group type ($P2_13$) as the Na-containing oxidonitridophosphates. Originally, the crystal structures were solved by direct methods but we also performed refinements using the atomic coordinates of $Na_3Ti(PO_3)_3N$ as a starting model. The results were the same, confirming that both structures are isostructural with $Na_3Ti(PO_3)_3N$ (as well as with all previously reported cubic oxionitridophosphates with the same formula type).

Acknowledgements

Any acknowledgements?

References

Allen, F. H., Johnson, O., Shields, G. P., Smith, B. R. & Towler, M. (2004). *J. Appl. Cryst.* **37**, 335–338.

Bang, S. Y., Khai, T. V., Oh, D. K., Maneeratanasarn, P., Choi, B. G., Ham, H. & Shim, K. B. (2013). J. Ceram. Process. Res. 14(S1), 74–76.

Blessing, R. H. (1995). *Acta Cryst.* A**51**, 33–38.

Brandenburg, K. (2006). *DIAMOND*. Crystal Impact GbR, Bonn, Germany.

Brese, N. E. & O'Keeffe, M. (1991). *Acta Cryst.* B**47**, 192–197.

Brown, I. D. & Altermatt, D. (1985). *Acta Cryst.* B**41**, 244–247.

Conanec, R., Feldmann, W., Marchand, R. & Laurent, Y. (1996). *J. Solid State Chem.* **121**, 418–422.

Conanec, R., l'Haridon, P., Feldmann, W., Marchand, R. & Laurent, Y. (1994). *Eur. J. Solid State Inorg. Chem.* **31**, 13–24.

Cosby, M. R., Mattei, G. S., Wang, Y., Li, Z., Bechtold, N., Chapman, K. W. & Khalifah, K. W. (2020). *J. Phys. Chem. C*, **124**, 6522–6527.

Farrugia, L. J. (2012). *J. Appl. Cryst.* **45**, 849–854.

Feldmann, W. (1987*a*). *Z. Chem.* **27**, 100–101.

Feldmann, W. (1987*b*). *Z. Chem.* **27**, 182–183.

Kim, J., Yoon, G., Lee, M. H., Kim, H., Lee, S. & Kang, K. (2017). *Chem. Mater.* **29**, 7826–7832.

Kim, M. & Kim, S.-J. (2013). *Acta Cryst.* E**69**, i34.

Liu, J., Chang, D., Whitfield, P., Janssen, Y., Yu, X., Zhou, Y., Bai, J., Ko, J., Nam, K.-W., Wu, L., Zhu, Y., Feygenson, M., Amatucci, G., Van der Ven, A., Yang, X.-Q. & Khalifah, P. (2014). *Chem. Mater.* **26**, 3295–3305.

Liu, J., Whitfield, P. S., Saccomanno, M. R., Bo, S.-H., Hu, E., Yu, X., Bai, J., Grey, C. P., Yang, X.-Q. & Khalifah, P. G. (2017). *J. Am. Chem. Soc.* **139**, 9192–9202.

Liu, J., Yin, L., Yang, X.-Q. & Khalifah, P. G. (2018). *Chem. Mater.* **30**, 4609–4616.

Liu, J., Yu, X., Hu, E., Nam, K.-W., Yang, X.-Q. & Khalifah, P. G. (2013). *Chem. Mater.* **25**, 3929–3931.

Massiot, D., Conanec, R., Feldmann, W., Marchand, R. & Laurent, Y. (1996). *Inorg. Chem.* **35**, 4957–4960.

Oxford Diffraction (2006). *CrysAlis CCD* and *CrysAlis RED*. Oxford Diffraction Ltd, Abingdon, England.

Parsons, S., Flack, H. D. & Wagner, T. (2013). *Acta Cryst.* B**69**, 249–259.

Reynaud, M., Wizner, A., Katcho, N. A., Loaiza, L. C., Galceran, M., Carrasco, J., Rojo, T., Armand, M. & Casas-Cabanas, M. (2017). *Electrochem. Commun.* **84**, 14–18.

Shannon, R. D. (1976). *Acta Cryst.* A**32**, 751–767.

Sheldrick, G. M. (2008). *Acta Cryst.* A**64**, 112–122.

Sheldrick, G. M. (2015). *Acta Cryst.* C**71**, 3–8.

Wang, A., Wang, C., Fu, L., Wong-Ng, W. & Lan, Y. (2017). *Nano-Micro Lett.* **9**, 47.

Wang, S., Li, H., Zhang, W., Zheng, J., Li, S., Hu, J., Lia, Y. & Zhang, Z. (2021). *ACS Appl. Energy Mater.* In the press. https://doi.org/10.1021/acsaem.1c02042.

Westrip, S. P. (2010). *J. Appl. Cryst.* **43**, 920–925.

Xiao, J., Hua, W. & Chen, M. (2021). *Nanotechnology*, **32**, 425404.

Zatovsky, I. V., Slobodyanik, N. S., Stratiychuk, D. A., Domasevitch, K. V., Sieler, J. & Rusanov, E. B. (2000). *Z. Naturforsch. Teil B*, **55**, 291–298.

Zatovsky, I. V., Vorobjova, T. V., Domasevitch, K. V., Ogorodnyk, I. V. & Slobodyanik, N. S. (2006). *Acta Cryst.* E**62**, i32–i34.

Zhang, H., Buchholz, D. & Passerini, S. (2017). *Energies*, **10**, 889.